Equilibrium Unfolding Studies of Barstar: Evidence for an Alternative Conformation Which Resembles a Molten Globule†

Ritu Khurana and Jayant B. Udgaonkar*

National Centre for Biological Sciences, TIFR Centre, P.O. Box 1234, Indian Institute of Science Campus, Bangalore 560 012, India

Received March 16, 1993; Revised Manuscript Received October 22, 1993®

ABSTRACT: The folding of the small protein barstar, which is the intracellular inhibitor to barnase in *Bacillus amyloliquefaciens*, has been studied by equilibrium unfolding methods. Barstar is shown to exist in two conformations: the A form, which exists at pH values lower than 4, and the N state, which exists at pH values above 5. The transition between the A form and the N state is completely reversible. UV absorbance spectroscopy, fluorescence spectroscopy, and circular dichroism spectroscopy were used to study the two conformations. The mean residue ellipticity measured at 220 nm of the A form is 60% that of the N state, and the A form has some of the properties expected for a molten globule conformation. Fluorescence energy transfer experiments using 1-anilino-8-naphthalenesulfonate indicate that at least one of the three tryptophan residues in the A form is accessible to water. Surprisingly, high concentrations of denaturant are required to unfold the A form. For denaturation by guanidine hydrochloride, the midpoint of the cooperative unfolding transition measured by circular dichroism for the A form at pH 3 is 3.7 ± 0.1 M, which is significantly higher than the value of 2.0 ± 0.1 M observed for the N state at pH 7. The unfolding of the A form by guanidine hydrochloride or urea is complex and cannot be satisfactorily fit to a two-state (A ⇌ U) model for unfolding. Fluorescence-monitored tertiary structure melts before circular dichroism-monitored secondary structure, and an equilibrium unfolding intermediate must be present on the unfolding pathway of A.

To determine how the information resident in the linear amino acid sequence of a protein is translated into a unique three-dimensional structure is an important problem in physical biochemistry. The unique, three-dimensional structure, which confers to a protein its specific function, is generally accepted to be the thermodynamically most stable conformation that can be adopted by a polypeptide chain. Nonetheless, it has become increasingly evident that a polypeptide chain can adopt conformations different from the functional, native conformation of the protein. The study of these partly folded conformations is important for an understanding of the principles governing protein folding (Baldwin, 1991; Dill & Shortle, 1991; Dobson, 1992).

The classic examples of such conformations are the molten globule conformations [reviewed by Kuwajima (1989), Baldwin (1991), and Ptitsyn (1992)] adopted by several proteins at extremes of pH and ionic strength (Goto et al., 1990a,b), typically at acidic pH. The molten globule conformation is a partly folded one: it is nearly as compact as the native conformation, although it has less secondary structure, more hydrated hydrophobic residues (Ptitsyn, 1987), and apparently no defined tertiary structure (Ewbank & Creighton, 1991). Other nonnative conformations that can be adopted by a polypeptide chain have also been described. α-Lytic protease, when refolded in the absence of the pro region of its inactive precursor, forms a structure with some of the characteristics of a molten globule (Baker et al., 1992). The immunoglobulin MAK33 assumes a conformation at acidic pH that possesses all of the characteristics of a molten globule but, in addition, also appears to be stabilized by tertiary interactions (Buchner et al., 1991).

Interest in molten globules is strong because the properties of the molten globule support the argument that it may be one of the first conformations embraced by the polypeptide chain in folding from the unfolded state (Kim & Baldwin, 1990; Baldwin, 1991). Early kinetic intermediates resembling molten globules have been seen for several proteins (Ptitsyn et al., 1990), including α-lactalbumin (Kuwajima, 1989), the β-subunit of tryptophan synthase (Goldberg et al., 1990), lysozyme (Radford et al., 1992), and cytochrome C (Elöve et al., 1992), but it still has not been unambiguously demonstrated that the molten globule is a general intermediate formed on the kinetic pathway of protein folding. Recent studies have shown that the structure of the polypeptide chain that is recognized by at least one chaperone protein is a structure resembling a molten globule (Martin et al., 1991), and consequently, it is the binding of the chaperone to this molten globule-like state that allows the polypeptide chain to remain in a state competent for folding to the functional native structure.

The study of alternatively folded, nonnative conformations like the molten globule is therefore of direct relevance to how proteins fold to their native conformations. We have been studying an alternative conformation of the small protein barstar that resembles a molten globule. Barstar is an 89 amino acid residue protein of molecular weight 10 100 produced naturally by *Bacillus amyloliquefaciens* (Hartley et al., 1972). It is an intracellular inhibitor of the ribonuclease, barnase, produced by the same organism; it binds barnase to form a 1:1 complex (Smeaton & Elliot, 1967; Hartley & Smeaton, 1973), with a dissociation constant in the picomolar region (U. Nath and J. B. Udgaonkar, unpublished results). It has no disulfide bonds and unfolds reversibly. Substantial progress has been made toward obtaining a solution structure of native barstar using two-dimensional proton NMR[1] techniques (Wüthrich, 1986): over one-half of the proton resonances in the NMR spectrum of barstar have been

† This work was funded by the Tata Institute of Fundamental Research and by the Department of Biotechnology, Government of India. J.B.U. is the recipient of a Biotechnology Career Fellowship from the Rockefeller Foundation.

® Abstract published in *Advance ACS Abstracts,* December 15, 1993.

0006-2960/94/0433-106$04.50/0

sequentially assigned (S. Ramachandran and J. B. Udgaonkar, unpublished results). Large amounts of barstar are available from an expression system in *Escherichia coli*, which uses a pUC19-based expression vector (Hartley, 1988). In every way, it is suited as a model protein for folding work. We report here our work on the characterization of the molten globule-like conformation of barstar. Surprisingly, this conformation (the A form) is found to unfold at substantially higher concentrations of denaturant than does the native conformation (the N state).

EXPERIMENTAL PROCEDURES

Purification of Barstar. The barstar expression plasmid pMT316, with the barstar structural gene under the control of the *tac* promoter inserted into the pUC19 plasmid, was obtained from Dr. R. W. Hartley (Hartley, 1988). Plasmid pMT316 was transformed into *E. coli* strain MM294.

A 100-mL overnight starter culture of pMT316/MM294 was used to inoculate 1 dm^3 of rich buffered medium (containing 12 g of bactotryptone, 24 g of yeast extract, 5 mL of glycerol, 12.2 g of potassium monohydrogen phosphate, and 2.4 g of potassium dihydrogen phosphate). Barstar production was induced 6 h after inoculation by the addition of 10 mg of IPTG, and the cells were harvested 16 h after induction. The intracellular barstar was extracted with a low-salt buffer (0.2 M ammonium acetate, 1 mM EDTA, 1 mM BME, and 0.5 mM PMSF at pH 8.0) after first lysing the cells using a French press cell at 4–5 atm of pressure. This was followed by ammonium sulfate precipitation, and barstar was obtained in the 40–80% cut. This was then passed through a G-75 Sephadex gel filtration column. Fractions containing barstar were pooled and purified further using anion-exchange chromatography on a DEAE Sephadex column. Barstar was eluted from the column using a high-salt buffer (0.8 M ammonium acetate, 1 mM EDTA, 1 mM BME, and 0.5 mM PMSF at pH 8.0). The eluted protein was desalted using an Amicon stirred ultrafiltration cell with a YM3 filter, concentrated to a volume of 5–10 mL, and then lyophilized. The activity of barstar at various steps of the purification procedure was followed by using a spectrophotometric assay, which monitored the inhibition of barnase (purified in our laboratory from plasmid pMT413, also obtained from Dr. R. W. Hartley) activity using Torula yeast RNA as the substrate (Mossakowska et al., 1989).

The purity of barstar was checked by tricine–sodium dodecyl sulfate–polyacrylamide gel electrophoresis using 16.5% T and 3% C separating gels (Schagger & von Jagow, 1987) and low molecular weight markers obtained from Bethesda Research Laboratories. The protein was found to be more than 98% pure. The yield of the purified protein was typically around 200 mg/L of *E. coli* culture. Protein concentration was determined by a colorimetric assay (Bradford, 1976), and the extinction coefficient of barstar was determined to be 23 000 M^{-1} cm^{-1} at 280 nm.

Spectroscopic Methods. Equilibrium unfolding as a function of denaturant concentration was monitored by three spectroscopic methods: (1) UV difference absorbance spectroscopy, where changes in absorbance over a wavelength range of 250–320 nm were measured by a Cary 1 spectrophotometer. (2) CD spectroscopy was done on a Jasco J600 spectropolarimeter. Secondary structure was monitored in the wavelength range 200–250 nm using a cell of 0.1 cm path length, and tertiary structure was monitored in the wavelength range 250–320 nm using a cell of path length 1 cm. For all measurements, a spectral bandwidth of 5 nm and a time constant of 1 s were used, and each spectrum was recorded as an average of 10 scans. Some CD data were collected on an Aviv 60 spectropolarimeter at Stanford University. (3) Fluorescence spectroscopy studies were done using a Shimadzu RF-540 spectrofluorimeter. For measurements of intrinsic protein fluorescence, the excitation wavelength used was 287 nm. Emission spectra were recorded with both excitation and emission slit widths set at 5 nm. A few measurements were made on a Perkin-Elmer MPF-44A fluorimeter at the Indian Institute of Science. All measurements were made at 25 °C.

Buffers, Denaturants, and Solutions. The buffers used for the spectroscopic measurements at different pH values were glycine (pH 2 and 3), sodium acetate (pH 4 and 5), MES (pH 6), sodium phosphate (pH 7), and sodium borate (pH 8 and 9), at concentrations of 20 mM. Buffer solutions were made by suitably mixing solutions of the acidic and basic forms of the buffers so as to obtain the desired pH. All buffers also contained 1 mM EDTA and 1 mM DTT. For some measurements, the buffers contained 0.2 M KCl. All buffer constituents were obtained from Sigma. Unfolding conditions were provided by the addition of 6 M GdnHCl, obtained from Sigma (molecular biology reagent grade), in the same buffers. For pH titration experiments using CD, a buffer mixture containing 10 mM sodium borate, 10 mM sodium citrate, 10 mM sodium phosphate, 1 mM EDTA, and 100 μM DTT was used, and the pH was adjusted to the desired value within the range 1.5–9 pH units by the addition of either 1 M HCl or 1 M NaOH. Other denaturants used were ultrapure GdnSCN from Bethesda Research Laboratories and ultrapure urea from Research Organics Inc. Stock solutions of urea were made fresh on the day of use. The concentrations of stock solutions of urea and GdnHCl were determined by measurement of the refractive index (Pace et al., 1989). For experiments in which the binding of ANS to barstar was studied, a 10 mM stock solution of ANS (obtained from Sigma) was prepared and filtered through a 0.45-μm filter, and the concentration was checked by using an extinction coefficient of 5000 M^{-1} cm^{-1} at 350 nm (Stryer, 1965). Protein concentrations used were typically 40 μM for absorbance and near-UV CD, 4 μM for fluorescence, and 20 μM for far-UV CD measurements.

Data Analysis. All data were analyzed using the nonlinear least-squares fitting routine in the SigmaPlot Scientific Graphing System, version 4.02, from Jandel Corporation.

The pH titration data were fit to the following equation:

$$Y(\mathrm{pH}) = \frac{Y_d + Y_p 10^{\mathrm{pH}-\mathrm{pH_m}}}{1 + 10^{\mathrm{pH}-\mathrm{pH_m}}} \quad (1)$$

where Y(pH) is the spectroscopic property being measured at a particular pH value, Y_d and Y_p are the spectroscopic properties characteristic of the deprotonated and protonated states respectively, and pH_m is the midpoint of the observed titration.

To obtain the value for C_M from an equilibrium solvent–denaturation curve, the regions of the curve preceding and following the cooperative part of the transition were first fit to straight lines. The straight lines were extrapolated to the

[1] Abbreviations: NMR, nuclear magnetic resonance; CD, circular dichroism; ANS, 1-anilino-8-naphthalenesulfonate; IPTG, isopropyl β-D-thiogalactopyranoside; BME, β-mercaptoethanol; DTT, dithiothreitol; EDTA, ethylenediaminetetraacetic acid; PMSF, phenylmethanesulfonyl fluoride; GdnHCl, guanidine hydrochloride; GdnSCN, guanidine isothiocyanate.

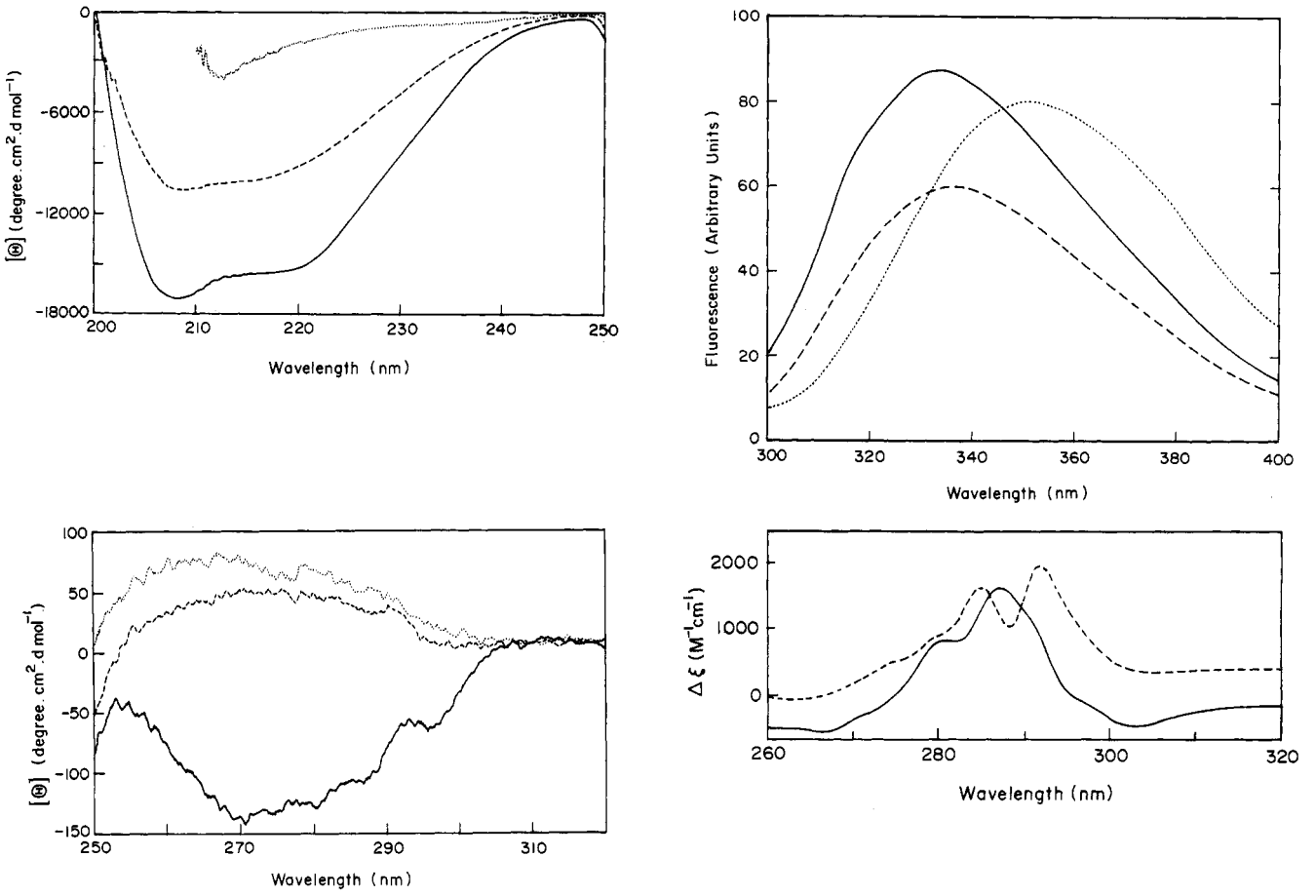

FIGURE 1: Spectroscopic characterization of barstar. CD, fluorescence, and absorbance spectra were recorded at pH 7 and pH 3 in both the presence (pH 7, ···) and absence (pH 7, —; pH 3, ---) of 6.0 M GdnHCl. (a, top left) Dependence of mean residue ellipticity on wavelength in the peptide region. (b, bottom left) Dependence of mean residue ellipticity on wavelength in the aromatic region. (c, top right) Fluorescence emission spectra on excitation at 287 nm. (d, bottom right) Difference UV absorbance spectra of barstar at both pH 7 (—) and pH 3 (---). The difference in molar extinction coefficients of the protein in the absence and presence of 6.0 M GdnHCl is plotted against wavelength.

cooperative part of the transition, and the C_M value was obtained as the concentration of denaturant at which the protein is half unfolded.

To obtain the value for T_g, the temperature at which the protein is half unfolded, from a thermal denaturation curve, the first derivative of the optical signal with respect to temperature was determined first, and T_g was determined as the value at which the first derivative exhibited a minimum value.

RESULTS

Spectroscopic Characterization of the N and A Forms of Barstar. CD spectra of the native (N), acid (A), and 6 M GdnHCl-denatured (U) states of barstar were recorded in the peptide region (far-UV region; Figure 1a) as well as the aromatic region (near-UV region; Figure 1b). The far-UV CD spectra of the N state and the A form show that both forms have considerable secondary structure, and the spectra are characteristic of proteins with α-helices. The mean residue ellipticities at 220 nm are -8600 ± 900 deg cm^2 dmol^{-1} for the A form, $-14\,600 \pm 1500$ deg cm^2 dmol^{-1} for the N state, and -1600 ± 170 deg cm^2 dmol^{-1} for the U state (both at pH 3 and at pH 7). The value for the U state is less than that expected (-2600 deg cm^2 dmol^{-1}) for a random conformation of a polypeptide chain (Chen et al., 1972), but this may be because the CD spectrum of the U state is affected by the presence of GdnHCl (Privalov et al., 1989). The near-UV CD spectrum of the A form is essentially absent in comparison to that of the N state, indicating that aromatic residues in the former are no longer in an asymmetric environment. The data in Figure 1a,b also rule out the possibility that at pH 3 barstar molecules exist in two populations, 60% N and 40% U, because in that case the near-UV spectral intensity would also be expected to be decreased to 60% in the A form.

To check the effect of the ionic strength of the buffer on the structures of both the A and N states, the ionic strength of the buffer was increased by the addition of KCl. Concentrations of KCl up to 0.2 M had no significant effect on the mean residue ellipticity measured at 220 nm. Increasing the concentration of KCl to 0.8 M did, however, increase the mean residue ellipticity at 220 nm for both the N and A forms by approximately 10% (data not shown). Increasing the ionic strength beyond 1.0 M was not possible because this limited the solubility of barstar.

The fluorescence emission spectra of the N, A, and U forms (Figure 1c) were collected by exciting the protein at 287 nm and are representative of proteins containing both tyrosine and tryptophan residues (barstar has three of each). The emission maximum for barstar in the N state is at 331 nm, whereas in the A form there is both a 40% decrease in the maximum fluorescence intensity and a red shift in the emission maximum by 5 nm. The U state, however, exhibits a much larger red shift with maximum emission occurring at 351 nm, which indicates that all of the tryptophan residues are fully

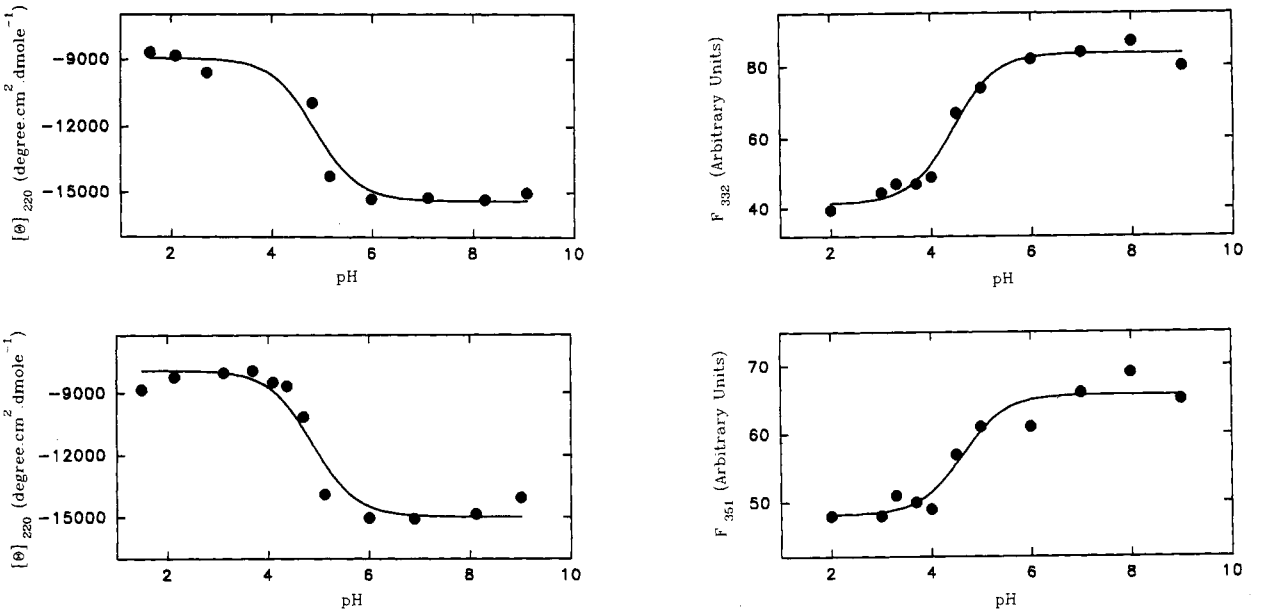

FIGURE 2: pH dependence of the conformation of barstar. (a, top left) The mean residue ellipticity at 220 nm, measured in the absence of GdnHCl, is plotted against pH. (b, bottom left) The mean residue ellipticity at 220 nm, measured in the presence of 1 M GdnHCl, is plotted against pH. (c, top right) The intensity of the fluorescence emission of barstar at 332 nm on excitation at 287 nm is plotted versus pH. (d, bottom right) The intensity of the fluorescence emission of barstar in 6.0 M GdnHCl, measured at 351 nm on excitation at 287 nm, is plotted versus pH. The solid lines through the data points were drawn according to eq 1. The concentrations of barstar used in the fluorescence and CD measurements were 4 and 30 μM, respectively.

exposed. The maximum fluorescence intensity of the A form is less than those of the N and U states.

UV absorbance spectra for the N, A, and U (at both pH 7 and pH 3) states were collected. The UV difference spectra in Figure 1d for the N and A forms of barstar show the differences in tertiary structure between N and U states and between the A and U states, respectively. The difference spectrum for the N state shows two peaks at 280 and 287 nm (a small hump at 292 nm can also be distinguished), while the difference spectrum for the A form manifests distinct peaks at 280, 285, and 292 nm. Unfolding of N is accompanied by a change in ϵ_{287} of 1650 ± 170 M^{-1} cm^{-1}, while unfolding of A is accompanied by a change in ϵ_{292} of 1990 ± 200 M^{-1} cm^{-1} and a change in ϵ_{285} of 1650 ± 170 $M^{-1}cm^{-1}$. There is virtually no difference between the absorbance spectra of the U state at pH 7 and at pH 3 between 260 and 300 nm.

To demonstrate that the difference in spectroscopic properties observed between the A form and the N state was not an experimental artifact caused by protein aggregation at low pH, the dependence of the spectroscopic property being studied on the concentration of barstar was studied at both pH 3 and pH 7 (data not shown). The fluorescence at 332 nm showed a linear dependence on the concentration of barstar in the range studied, 0.6–6 μM, and the mean residue ellipticity at 220 nm showed a linear dependence on the concentration of barstar in the range studied, 3–60 μM, at both pH 3 and pH 7. All spectroscopic measurements were made within the linear range of barstar concentration.

pH Titrations. The mean residue ellipticity and fluorescence of barstar were measured as functions of pH in the range 1.5–9. Figure 2a,b illustrates the effect of pH on the mean residue ellipticity at 220 nm, both in the absence (Figure 2a) and presence (Figure 2b) of 1 M GdnHCl; fits of the data to eq 1 yield values for pH_m of 4.8 ± 0.2. A similar pH titration monitoring the effect of pH on the fluorescence emission of barstar at 332 nm is shown in Figure 2c, and a fit of these data to eq 1 yields a value for pH_m of 4.4 ± 0.2. When the wavelength of maximum fluorescence was plotted versus pH (data not shown), a titration with a similar pH_m value was obtained. In both the CD and the fluorescence experiments, the transition between the A form and the N state appears to follow the titration of a single ionizable group (the data fit well to eq 1); moreover, pH-jump experiments showed that it is completely reversible.

The wavelength of maximum emission of barstar in the U state (in the presence of 6 M GdnHCl) remained at 351 nm over the pH range 2–9. The fluorescence intensity di , however, increase with an increase in pH from 2 to 9 (Figure 2d). As in the case of the data in Figure 2c, the data in Figure 2d indicate the titration of one ionizable group and are characterized by a pH_m of 4.6. In the presence of 6 M GdnHCl, the change in fluorescence intensity over the titration is only approximately 40% of that in the absence of GdnHCl.

ANS Binding. Figure 3a shows that the addition of ANS to the A form of barstar (at pH 3) results in an increase in ANS fluorescence, while the addition of ANS to the N state (at pH 7) does not lead to a significant rise in ANS fluorescence. No increase in ANS fluorescence is seen when ANS is added to completely unfolded barstar (in 6 M GdnHCl) at pH 7 or 3 (data not shown). The binding of ANS to the A form of barstar also leads to a shift of the emission maximum of ANS from 530 to 470 nm.

Figure 3b shows the results of fluorescence energy transfer experiments performed to characterize further the binding of ANS to the A form of barstar. The excitation spectrum of ANS and the fluorescence emission spectrum of the tryptophans in barstar show considerable overlap. When the barstar tryptophans are excited at 287 nm, it is observed that the protein fluorescence decreases with an increase in ANS concentration and that there is a concomitant increase in ANS fluorescence. At the maximum concentration of ANS used in these experiments, the inner-filter effect caused by absorption by ANS at the excitation wavelength can be ignored.

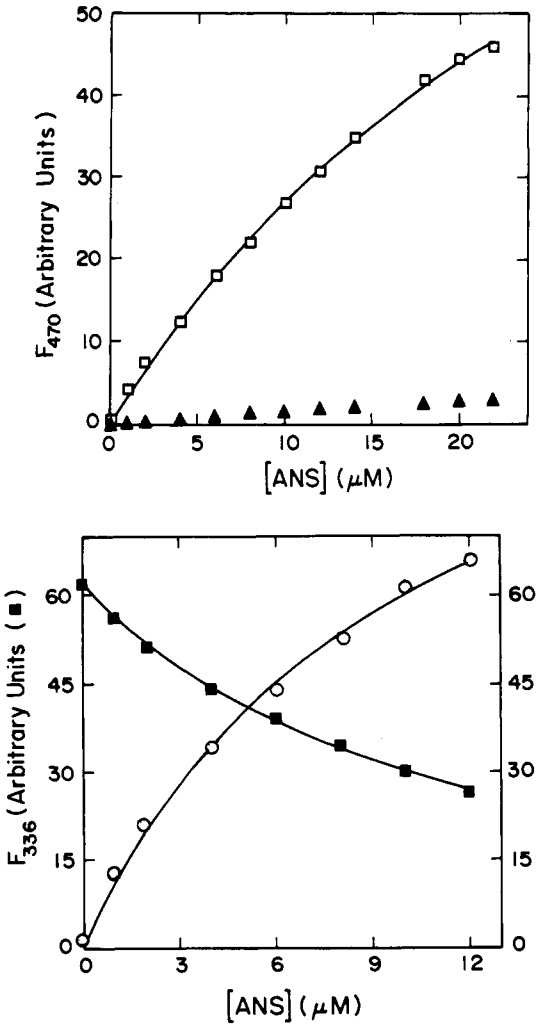

FIGURE 3: ANS binding. (a, top) The change in intensity of ANS fluorescence (ΔF) at 470 nm on excitation at 380 nm is plotted versus ANS concentration. The concentration of barstar used was 1 μM: (▲) pH 7; (□) pH 3. (b, bottom) Fluorescence energy transfer. Intrinsic tryptophan fluorescence of barstar at 336 nm (■) and ANS fluorescence at 470 nm (○) are plotted versus ANS concentration. The concentration of barstar used was 1 μM, and the excitation wavelength was 287 nm. The solid lines through the data are nonlinear least-squares fits to eq 2 (see text). The values for the binding parameters obtained are n = 1.1, K_D = 11 μM (protein tryptophan fluorescence data) and n = 1.2, K_D = 10 μM (ANS fluorescence data).

The data in Figure 3b were fit to

$$\Delta F(L) = n\Delta F_{max}\frac{[L]}{[L] + K_D} \quad (2)$$

where n is the number of identical, noninteracting binding sites for ANS on the A form of barstar, and K_D is the dissociation constant for ANS binding to the protein. $\Delta F(L)$ is the change in fluorescence on the addition of ANS at a concentration [L], and ΔF_{max} is the change in fluorescence measured when all of the barstar is complexed with ANS. Both sets of data in Figure 3b could be fit well to eq 2, and they indicate that there is one binding site for ANS on each molecule of barstar in the A form to which ANS binds with a dissociation constant of approximately 11 μM (see Figure 3b legend).

Equilibrium Unfolding of the N and A Forms of Barstar. The unfolding transitions of the N and A forms of barstar were studied by monitoring the fluorescence at 322 nm (the wavelength at which the difference in fluorescence emission between the N and U states is a maximum; see Figure 1c) on excitation at 287 nm and by monitoring the mean residue ellipticity at 220 nm. The former represents a measure of the tertiary structure, while the latter measures secondary structure. The unfolding of the A form was followed by monitoring the absorbance at 292 nm as well, which also serves as a probe of tertiary structure.

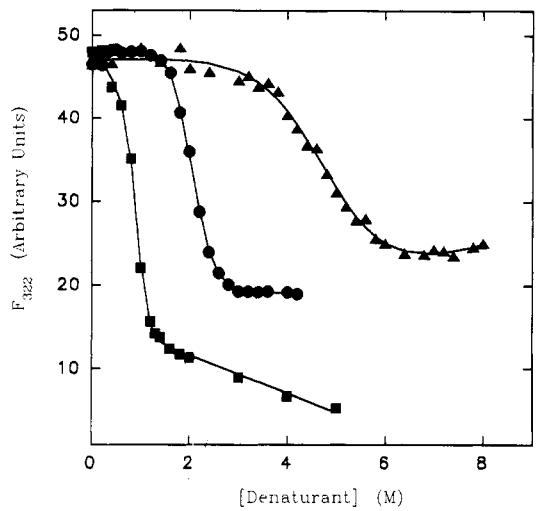

FIGURE 4: Equilibrium unfolding of barstar at pH 7. The unfolding transition was monitored by fluorescence at 322 nm for (●) GdnHCl, (▲) urea, and (■) GdnSCN induced transition. The solid lines through the data have been drawn by inspection only.

In Figure 4 are shown the equilibrium unfolding transitions for barstar in the N state at pH 7 using three denaturants, GdnHCl, urea, and GdnSCN, and fluorescence as the probe of folding. In the case of each of the three denaturants, the unfolding curve shows a single, smooth cooperative transition. In the case of the urea denaturation curve, it is observed that the intrinsic fluorescence intensity of unfolded barstar increases with an increase in urea concentration beyond 7 M, which is the expected behavior because it has been shown that the fluorescence of both tryptophan and tyrosine increases with urea concentration (Schmid, 1989). The concentration of denaturant at which barstar is half unfolded, C_M, is 2.0 ± 0.1 M for GdnHCl, 4.7 ± 0.1 M for urea, and 0.9 ± 0.1 M for GdnSCN. When mean residue ellipticity was used as a probe for unfolding by GdnHCl, the value for C_M, 2.0 ± 0.1, was the same as the value obtained using fluorescence as the probe (results not shown). The unfolding transition was complete within 3 h; after 24 h of equilibration, identical unfolding curves were obtained. The transition was also completely reversible. If barstar was first completely unfolded in 6 M GdnHCl and then allowed to equilibrate at lower denaturant concentrations within the transition zone, the refolding transition followed the unfolding transition (data not shown).

The GdnHCl denaturation curves obtained for the A form at pH 3 are shown in Figure 5. It was observed that the slope of the base line in the folded region of the denaturation curve was large when monitored by fluorescence (Figure 5a), CD (Figure 5b), or absorbance (Figure 5c), especially in comparison to the denaturation curves obtained for the N state at pH 7. The steepness of the base line preceding the cooperative unfolding transition indicates a partial melting of structure at low GdnHCl concentrations, which precedes the cooperative unfolding transition at higher GdnHCl concentrations. The absorbance and CD-monitored denaturation curves yielded similar values for C_M (3.7 ± 0.1 M) for the cooperative unfolding transition, while the fluorescence-

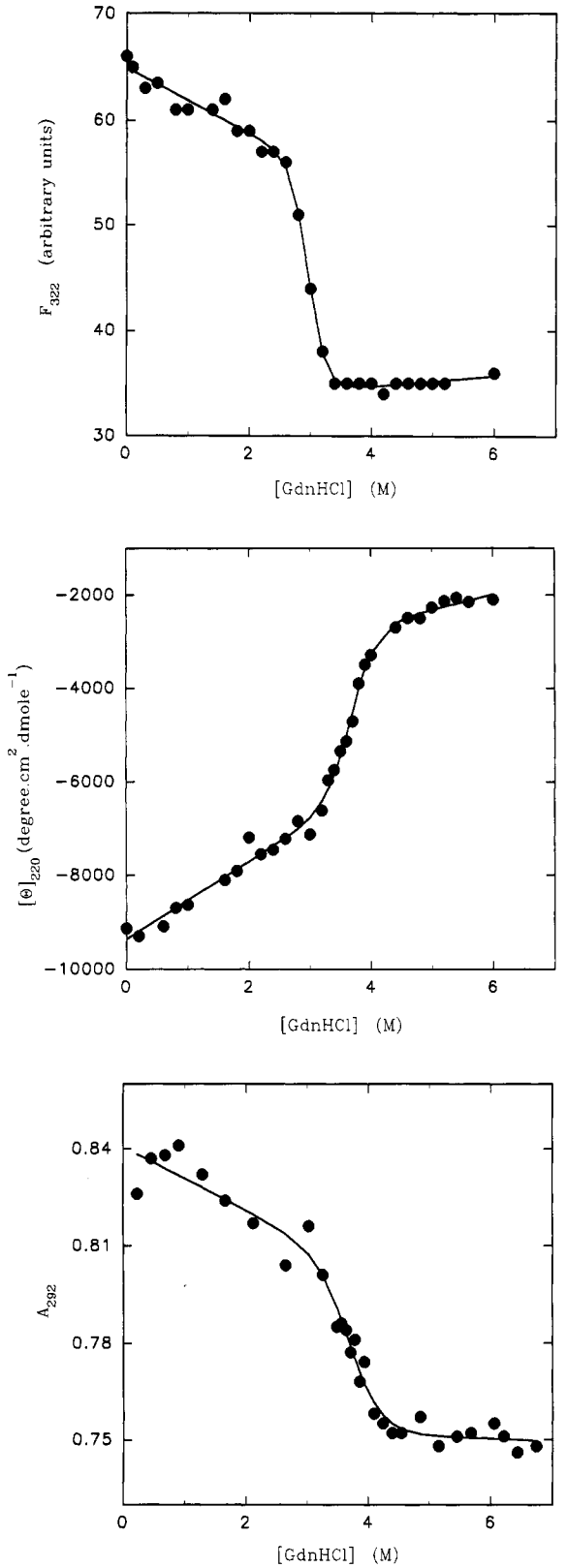

FIGURE 5: Equilibrium unfolding transitions of the A form of barstar at pH 3. Unfolding was monitored by measuring (a, top) the fluorescence at 322 nm on excitation at 287 nm, (b, middle) the mean residue ellipticity at 220 nm, and (c, bottom) the absorbance at 292 nm. The protein concentration was 4 μM for the fluorescence measurements and 40 μM for the ellipticity and absorbance measurements. The solid lines have been drawn by inspection only.

monitored denaturation curve yielded a lower value for C_M (3.1 ± 0.1 M).

An increase in ionic strength by including 0.2 M KCl in the sample buffers results in a much lower slope of the base line in the folded region of the denaturation curve: there is less partial melting of structure at low GdnHCl concentrations. This is seen for both fluorescence-monitored (Figure 6a) and CD-monitored (Figure 6b) unfolding. The values obtained for C_M in the presence of 0.2 M KCl (see the legend to Figure 6) are similar to the values obtained in its absence (see Figures 4 and 5 and text above). At pH 7, the C_M value is the same whether fluorescence or CD is used to monitor folding, whereas at pH 3 fluorescence-monitored unfolding precedes CD-monitored unfolding.

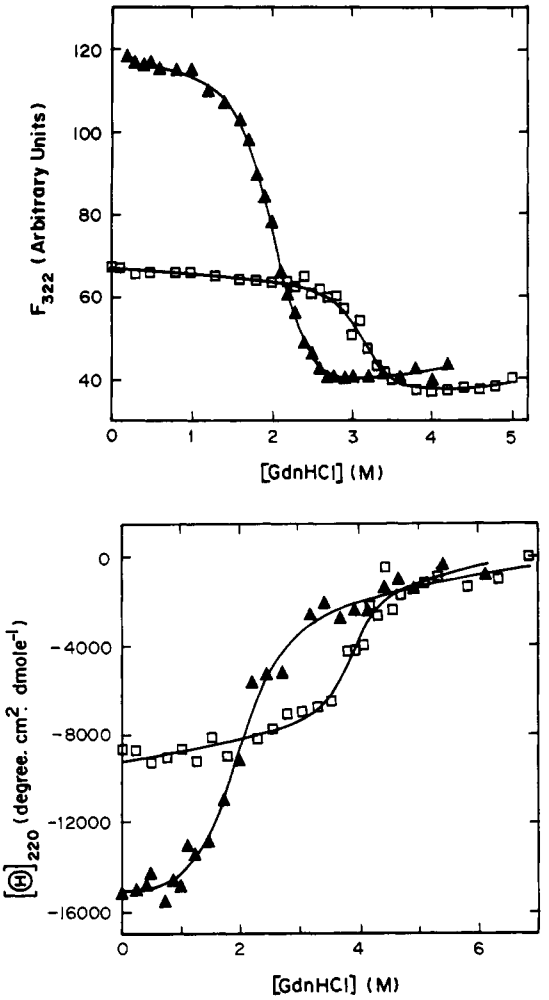

FIGURE 6: Equilibrium denaturation of barstar in the N state at pH 7 (▲) and the A form at pH 3 (□). Unfolding was followed by monitoring the fluorescence at 322 nm (a, top) and the mean residue ellipticity at 220 nm (b, bottom). All samples contained 0.2 M KCl. The solid lines through the data were drawn by inspection only. The C_M values obtained for the fluorescence-monitored denaturation curves are 2.0 ± 0.1 (pH 7) and 3.1 ± 0.1 (pH 3), while the CD-monitored denaturation curves yielded values for C_M of 1.9 ± 0.1 (pH 7) and 3.7 ± 0.1 (pH 3).

Figure 7 shows urea denaturation curves for the A form of barstar at pH 3, in the presence of 0.2 M KCl. The absorbance-monitored and CD-monitored denaturation curves are non-coincident, and in both, nearly 40% of the decrease in the optical signal monitoring unfolding occurs between 0 and 6 M urea, with the remaining part of the signal decreasing in a more cooperative unfolding transition between 6 and 9 M urea. At pH 7, the urea denaturation curve for the N state in the presence of 0.2 M KCl, obtained using fluorescence as the probe for folding, yielded a value for C_M of 4.7 ± 0.1 M (data not shown), which is the same as the value obtained in the absence of KCl (Figure 4).

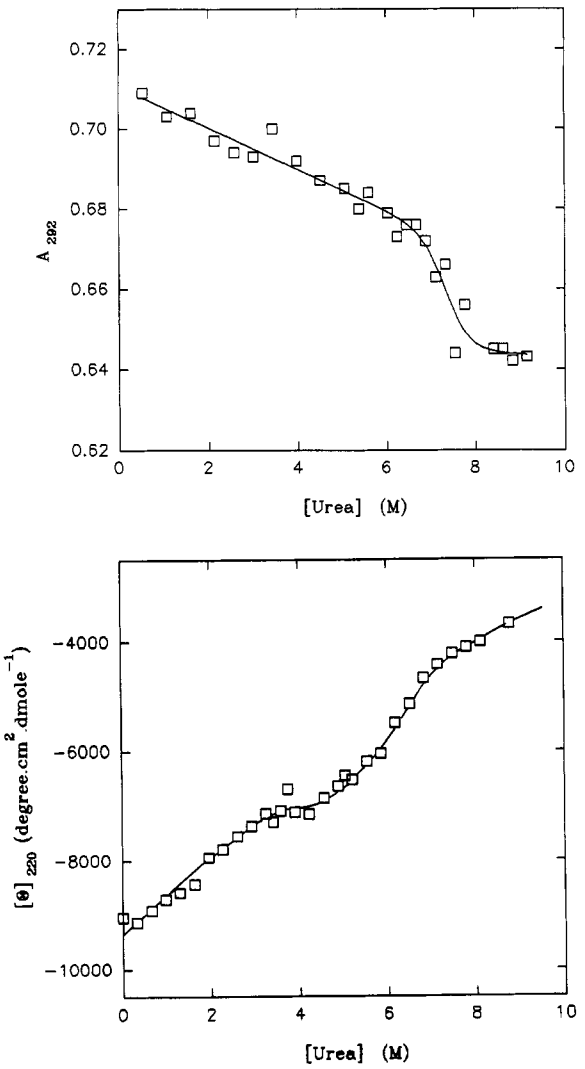

FIGURE 7: Urea denaturation of the A form. The unfolding of barstar at pH 3 by urea was followed by monitoring the absorbance at 292 nm (a, top) and the mean residue ellipticity at 220 nm (b, bottom). The solid lines through the data were drawn by inspection only.

Thermal Denaturation of Barstar. Thermal denaturation curves for barstar were obtained by heating the protein and measuring the mean residue ellipticity at 2-deg intervals. The sample was allowed to equilibrate for 6 min at each temperature before measurement. Such a curve for the N state is shown in Figure 8. The unfolding transition was only 80% reversible, presumably because of the long time (>2 h) spent by the sample at temperatures greater than 70 °C. Nearly all of the original spectroscopic signal could, however, be recovered at the end of a temperature ramp, if faster heating rates were employed and the sample was immediately cooled at the end of the ramp. The N state melts at a temperature, T_g, of 72 °C. The thermally unfolded state at pH 7 still shows residual secondary structure: the mean residue ellipticity is not zero, but has a value of −6600 deg cm^2 dmol^{-1}. The thermal denaturation data obtained for the A form at pH 3 did not show any transition up to 98 °C. The amount of secondary structure seen in the A form is more than that seen in thermally denatured barstar at pH 7.

DISCUSSION

There is considerable current interest in the study of partly folded states that can be adopted by a polypeptide chain under

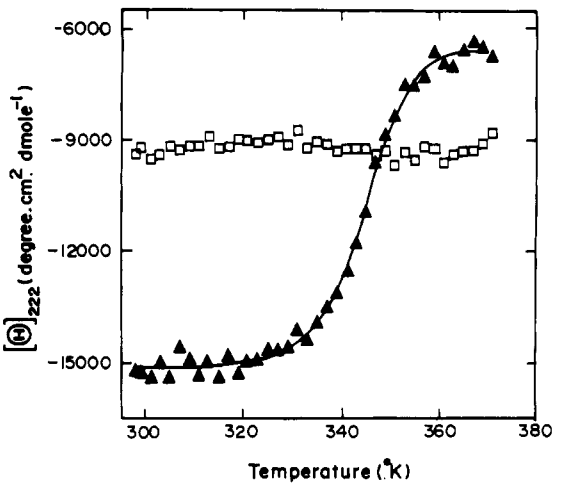

FIGURE 8: Thermal denaturation curves. Unfolding was monitored by measuring the mean residue ellipticity at 222 nm at pH 7 (▲) and pH 3 (□). Barstar (at 5 μM concentration) was dissolved in 5 mM sodium phosphate (pH 7) or 5 mM glycine (pH 3), 1 mM EDTA, and 100 μM DTT. The solid line through the data at pH 7 was drawn by inspection only.

equilibrium conditions (Baldwin, 1991; Dill & Shortle, 1991; Dobson, 1992). In part, the interest has arisen from the recognition that such states are similar to the partly folded kinetic intermediates that form on the folding pathway (Kim & Baldwin, 1990; Udgaonkar & Baldwin, 1988), but that are difficult to study in detail because of their transient nature. In particular, interest has focused on acid-denatured proteins and thermally denatured proteins which, in many cases, possess residual structure (Aune et al., 1967; Tanford, 1968) that disappears on further denaturation by high concentrations of urea or GdnHCl. More recently, it has been observed experimentally (Goto et al., 1990a; Jeng & Englander, 1991), as well as predicted theoretically (Finkelstein & Shakhnovich, 1989; Stigter et al., 1991), that acid denaturation of proteins can lead to at least two partly folded collapsed states, one open and the other more ordered and compact. The more extended open form transforms into the more ordered form, often referred to as the molten globule or the A form, with increasing ionic strength, as seen in the case of cytochrome C (Goto & Nishikori, 1991; Jeng et al., 1990; Jeng & Englander, 1991) and β-lactamase (Goto & Fink, 1989). In the case of the archetypal molten globule protein, α-lactalbumin, the molten globule form is seen even at low ionic strength (Kuwajima, 1989).

Barstar exists in an alternative conformation at low pH and ionic strength that resembles a molten globule. This alternative conformation is seen to unfold by a complex mechanism in which secondary structure melts after the tertiary structure. Barstar is therefore an attractive system to use for the study of the nature of the interactions that stabilize secondary structure in partly folded conformations of proteins.

Spectroscopic Characterization of Barstar. Upon acidification, the reversible transformation from the N state of barstar to the alternative A form is accompanied by a loss of approximately 40% of the mean residue ellipticity at 220 nm (Figure 1a). Since aromatic residues and sulfhydryl groups can also contribute to the mean residue ellipticity at 220 nm, this may not reflect the true content of secondary structure. In fact, the near-UV CD spectra (Figure 1b), the fluorescence emission spectra (Figure 1c), and the UV absorbance difference spectra (Figure 1d) all indicate that the environments of the aromatic residues in the A form significantly differ from those in the N state.

The dearth of structure discernible in the near-UV CD spectrum of the A form, in contrast to that seen for the N state (Figure 1b), is a characteristic feature of a molten globule state (Kuwajima, 1989). The similarity of the A form of barstar to such a state is further supported by the fluorescence emission spectra (Figure 1c). The wavelength of maximum emission for the A form (336 nm) is between those for the N state (331 nm) and the U state (351 nm). At least one of the three tryptophans of barstar is therefore more hydrated in the A form than in the N state. This increased degree of hydration of hydrophobic residues, which is another characteristic feature of molten globule states, is confirmed by ANS-binding experiments.

ANS is widely used as a probe for hydrated hydrophobic surfaces in proteins (Stryer, 1965). It has been used to detect the formation of molten globule-like intermediates on the folding pathways of several proteins (Ptitsyn et al., 1990). The binding of ANS to a hydrophobic surface or cluster results in a large increase in the fluorescence of the ANS as well as a blue shift in its emission maximum from 530 to 470 nm. These two effects are seen only with the A form at pH 3 and not with the N state at pH 7 (Figure 3a), indicating that the A form of barstar has hydrated hydrophobic surfaces or clusters that are absent from the N state.

The UV difference absorbance spectrum for the N state at pH 7 (Figure 1d) does not show a distinct peak at 292 nm (although a small hump on the spectrum can be discerned), while the corresponding spectrum for the A form does. This again suggests that the tryptophan residues in the N state are in local environments different from those in the A form. The blue shift in the tyrosine peak from 287 nm in the N state to 285 nm in the A form indicates greater solvent exposure of a tyrosine residue in the A form over the N state.

Thus, the CD, fluorescence, and UV absorbance spectroscopic studies, together with the ANS-binding studies, all indicate that the A form of barstar not only is distinct from the native state but that it also has several of the prominent features that characterize a molten globule.

The transition between the N and A forms is completely reversible and appears to be coupled to the titration of a single ionizable group with an apparent pK_a (as given by the midpoints of the titrations in Figure 2a–c) of 4.6 ± 0.2. The pH_m does not correspond to the true pK_a value of the titratable group because the protonation–deprotonation of this group is coupled to the transition between the N and A forms (Anderson et al., 1991). Thus, the apparent pK_a value depends on the equilibrium constant, K_{AN}, which characterizes the equilibrium between the A and N forms under conditions where both are deprotonated (e.g., at pH 8), and also on the true pK_a values of the titrating group in both the N state and the A form. The present data are insufficient to deduce the identity of the titratable group. Although the isoelectric point of barstar is 5.1 (R. Khurana and J. B. Udgaonkar, unpublished observations), it is unlikely that the transition corresponds to the net charge on the protein changing from a negative value for the N state at high pH to a positive value for the A form at low pH, because the data do appear to follow the titration of only one group.

The persistence of the pH titration monitored by fluorescence, even in the presence of 6 M GdnHCl (Figure 2d), can be explained on the basis of quenching of the fluorescence of a tryptophan residue by a titrating group adjacent to it in sequence (e.g., tryptophan 38 is next to aspartate 39). The pK_a values of titratable groups in proteins are essentially unaffected by the presence of 6 M GdnHCl (Nozaki & Tanford, 1967), and the similarity in the apparent pK_a values in the presence and absence of 6 M GdnHCl would suggest similar mechanisms for quenching of fluorescence at low pH. The change in fluorescence in the titration that is observed in the absence of 6 M GdnHCl is, however, nearly 2.5-fold greater than that observed in the presence of 6 M GdnHCl, and therefore invocation of only a local quenching process cannot fully explain the pH titration observed for the N to A transition. In fact, the titration from the N state to the A form is also accompanied by a red shift in the emission maximum of 5 nm (see above), indicating that, in addition to local quenching of tryptophan fluorescence, the solvent exposure of the tryptophan residues must be increasing in the transition from the N state to the A form. It is unlikely that a similar pH-dependent change in the solvent exposure of tryptophan residues also occurs in the presence of 6 M GdnHCl, because in the titration done in the presence of 6 M GdnHCl, the emission maximum remains at 351 nm (see Results).

Stability of the A and N States. Surprisingly, the A form of barstar unfolds at higher concentrations of denaturant at pH 3 than does the functional native N state at pH 7 (Figures 4, 5, 6, and 8). In the GdnHCl denaturation data obtained in the absence of KCl (Figures 4 and 5), this is reflected in the C_M values (2.0 ± 0.1 M for the N state versus 3.7 ± 0.1 M for the A form). This basic and important result is confirmed by similar measurements made in the presence of 0.2 M KCl (see the legend to Figure 6) and by urea denaturation experiments (Figures 1 and 7; see Results). In contrast, the molten globule form (acid form) of carbonic anhydrase B (Ptitsyn, 1992) melts at a lower concentration of denaturant than does the native state.

The complexity of the unfolding transition of the A state is seen especially for denaturation data obtained at low ionic strength (Figure 5) where a cooperative unfolding transition at high denaturant concentration is preceded by gradual melting at low denaturant concentration. In GdnHCl denaturation curves obtained for the A form (Figures 5 and 6), the fluorescence-monitored tertiary structure (C_M = 3.1 ± 0.1 M) melts before the CD-monitored secondary structure (C_M = 3.7 ± 0.1 M). The C_M for denaturation measured by absorbance is, however, the same as that measured by CD. The situation is therefore complex, with one probe of tertiary structure, fluorescence, showing denaturation to be occurring before another probe, absorbance. In the urea denaturation curves, nearly 40% of the optical signal change that monitors unfolding occurs gradually at low denaturant concentrations, and even the absorbance-monitored and CD-monitored denaturation curves are not coincident. Non-coincidence of denaturation curves monitored by different optical probes suggests the existence of equilibrium unfolding intermediates (Kim & Baldwin, 1990). Thus, at least one equilibrium unfolding intermediate (I_A) must be formed when the A form is denatured by GdnHCl. In the absence of detailed knowledge about the optical properties of the I_A form, however, it is not possible at the present time to quantitatively analyze the denaturation curves of the A form according to a three-state $A \rightleftharpoons I_A \rightleftharpoons U$ mechanism for unfolding, as has been possible for other proteins (Kuroda et al., 1992; Kuwajima et al., 1976).

It is not clear why an increase in ionic strength by the addition of 0.2 M KCl has such a striking effect on the partial melting of structure that precedes the cooperative transition seen in the denaturation curve of the A form (Figures 5 and 6). There is no significant effect on the amount of secondary structure in the A form in the absence of denaturant, but in

the presence of denaturant, the decrease in hydrophobic interactions caused by the denaturant is probably counteracted either by the increase in hydrophobic interactions caused by the addition of salt or, alternatively, by the screening of repulsive positive charges by the added salt (Goto & Nishikiori, 1991). An increase in the ionic strength has been shown to have a dramatic effect on the two acid-denatured conformations of cytochrome C, both of which have nativelike secondary structure. The structure in the open denatured form, which forms at low ionic strength, is less specific and stable, as measured by amide hydrogen exchange, than in the molten globule form, which forms at high ionic strength (Jeng et al., 1990; Jeng & Englander, 1991).

The nature of the residual secondary structure seen in thermally unfolded barstar (Figure 8) at pH 7 or in the A form (Figures 1 and 8) is unclear. Residual secondary structure seen in thermally denatured ribonuclease A (Robertson & Baldwin, 1990) and lysozyme (Evans et al., 1991) does not appear to be specific and stable from amide hydrogen exchange experiments, but clustering of hydrophobic residues is suspected to occur in the latter case. Calorimetric measurements on α-lactalbumin have indicated that the degrees of hydration of hydrophobic residues are similar in the molten globule form (Pfeil et al., 1986), the thermally denatured form (Pfeil & Privalov, 1976), and the form present in 6 M GdnHCl. Thus, the structures of both partly folded conformations of barstar, the A form and thermally denatured barstar, may be similar, and both may be stabilized by hydrophobic interactions. It is also conceivable that tertiary interactions are important in stabilizing the secondary structure of the A form. Tertiary interactions have been implicated in stabilizing the acid-denatured conformation of the MAK33 antibody (Buchner et al., 1991), but in neither that case nor the case of barstar is there any evidence yet of specific tertiary interactions.

We have shown that barstar can exist in an alternative conformation, the A form at low pH. Surprisingly, higher concentrations of denaturant (GdnHCl or urea) are required to unfold the A form at pH 3 than the N state at pH 7, even though the former possesses less secondary structure, as detected by CD. The small size of barstar, the sizeable helix content of the A form, as suggested by its far-UV CD spectrum, and the complexity of the unfolding transition of the A form make it an interesting protein for further study. It is important to gain an understanding of the structural basis for the stability of the A form. It remains to be seen whether the secondary structure seen in the A form of barstar is nativelike, as in the case of the molten globule forms of α-lactalbumin (Baum et al., 1989), apomyoglobin (Hughson et al., 1990), cytochrome C (Jeng et al., 1990), and ubiquitin (Harding et al., 1991), or whether it is nonnative, as in the case of partly folded kinetic intermediates that form on the folding pathways of β-lactoglobulin (Sugawara et al., 1991) and lysozyme (Radford et al., 1992). Fortunately, the A form is sufficiently soluble in water at low pH to permit a structural characterization by two-dimensional NMR experiments, and such work is now in progress in our laboratory.

ACKNOWLEDGMENT

We are grateful to R. W. Hartley for his generous gift of the barstar and barnase expression systems and for his suggestions regarding the purification of barstar. We thank R. L. Baldwin, D. Barrick, M. K. Mathew, G. Krishnamoorthy, and K. S. Krishnan for useful discussions and for their comments on the manuscript.

REFERENCES

Anderson, D. E., Becktel, W., & Dahlquist, F. W. (1990) *Biochemistry 29*, 2403–2408.
Aune, K. C., Salahuddin, A., Zarlengo, M. H., & Tanford, C. (1967) *J. Biol. Chem. 242*, 4486–4489.
Baker, D., Sohl, J. I., & Agard, D. A. (1992) *Nature 356*, 263–265.
Baldwin, R. L. (1991) *Chemtracts 2*, 379–389.
Baum, J., Dobson, C. M., Evans, P. A., & Hanley, C. (1989) *Biochemistry 28*, 7–13.
Bradford, M. M. (1976) *Anal. Biochem. 72*, 248–254.
Buchner, J., Renner, M., Lilie, H., Hinz, H. J., Jaenicke, R., Kiefhaber, T., & Rudolph, R. (1991) *Biochemistry 30*, 6922–6929.
Chen, Y. H., Yang, J. T., & Martinez, J. T. (1972) *Biochemistry 11*, 4120–4131.
Dill, K. A., & Shortle, D. (1991) *Annu. Rev. Biochem. 60*, 795–825.
Dobson, C. M. (1992) *Curr. Opin. Struct. Biol. 2*, 6–12.
Elöve, G. A., Chaffotte, A. F., Roder, H., & Goldberg, M. E. (1992) *Biochemistry 31*, 6876–6843.
Evans, P. A., Topping, K. D., Woolfson, D. N., & Dobson, C. M. (1991) *Proteins: Struct., Funct., Genet. 9*, 248–266.
Ewbank, J. J., & Creighton, T. E. (1991) *Nature 350*, 518–520.
Finkelstein, A. V., & Shakhnovich, E. I. (1989) *Biopolymers 28*, 1681–1694.
Goldberg, M. E., Semisotnov, G. B., Friguet, B., Kuwajima, K., Ptitsyn, O. B., & Sugai, S. (1990) *FEBS Lett. 263*, 51–56.
Goto, Y., & Fink, A. L. (1989) *Biochemistry 28*, 945–952.
Goto, Y., & Nishikiori, S. (1991) *J. Mol. Biol. 222*, 679–686.
Goto, Y., Calciano, L. J., & Fink, A. L. (1990a) *Proc. Natl. Acad. Sci. U.S.A. 87*, 573–577.
Goto, Y., Takahashi, N., & Fink, A. L. (1990b) *Biochemistry 29*, 3480–3488.
Harding, M. M., Williams, D. H., & Woolfson, D. N. (1991) *Biochemistry 30*, 3120–3128.
Hartley, R. W. (1988) *J. Mol. Biol. 202*, 913–915.
Hartley, R. W., & Smeaton, J. R. (1973) *J. Biol. Chem. 248*, 5624–5626.
Hartley, R. W., Rogerson, D. L., & Smeaton, J. R. (1972) *Prep. Biochem. 2*, 243–250.
Hughson, F. M., Wright, P. E., & Baldwin, R. L. (1990) *Science 249*, 1544–1548.
Jeng, M. F., & Englander, S. W. (1991) *J. Mol. Biol. 221*, 1045–1061.
Jeng, M. F., Englander, S. W., Elöve, G. A., Wand, A. J., & Roder, H. (1990) *Biochemistry 29*, 10433–10437.
Kim, P. S., & Baldwin, R. L. (1990) *Annu. Rev. Biochem. 59*, 631–660.
Kuroda, Y., Kidokoro, S., & Wada, A. (1992) *J. Mol. Biol. 223*, 1139–1153.
Kuwajima, K. (1989) *Proteins: Struct., Funct., Genet. 6*, 87–103.
Kuwajima, K., Nitta, K., Yoneyama, M., & Sugai, S. (1976) *J. Mol. Biol. 106*, 359–373.
Makhatadze, G. I., & Privalov, P. L. (1992) *J. Mol. Biol. 226*, 491–505.
Martin, J., Langer, T., Boteva, R., Schramel, A., Horvich, A. L., & Hart, F. U. (1991) *Nature 352*, 36–42.
Mossakowska, D. E., Nyberg, K., & Fersht, A. R. (1989) *Biochemistry 28*, 3843–3850.
Nozaki, Y., & Tanford, C. (1967) *J. Am. Chem Soc.* 89, 736–742.
Pace, C. N., Shirley, B. A., & Thomson, J. A. (1989) in *Protein Structure: A Practical Approach* (Creighton, T. E., Ed.) pp 311–330, IRL Press, Oxford, U.K.
Pfeil, W., & Privalov, P. L. (1976) *Biophys. Chem. 4*, 33–40.
Pfeil, W., Bychkova, V. E., & Ptitsyn, O. B. (1986) *FEBS Lett. 198*, 287–291.

Privalov, P. L., Tiktopolu, E. I., Venyaminov, S. Yu., Venyaminov, Yu. V., Makhatadze, G. I., & Khechinashvili, N. N. (1989) *J. Mol. Biol. 205*, 737–750.
Ptitsyn, O. B. (1987) *J. Protein Chem. 6*, 273–293.
Ptitsyn, O. B. (1992) in *Protein Folding* (Creighton, T. E., Ed.) pp 243–300, W. H. Freeman, New York.
Ptitsyn, O. B., Pain, R. H., Semisotnov, G. V., Zerovnik, E., & Razgulyaev, O. I. (1990) *FEBS Lett. 262*, 20–24.
Radford, S. E., Dobson, C. M., & Evans, P. A. (1992) *Nature 358*, 302–307.
Robertson, A. D., & Baldwin, R. L. (1991) *Biochemistry 30*, 9907–9914.
Roder, H., Elöve, G. A., & Englander, S. W (1988) *Nature 335*, 700–704.
Schagger, H., & von Jagow, G. (1987) *Anal. Biochem. 166*, 368–379.
Schellman, J. A. (1978) *Bioplymers 17*, 1305–1322.
Schmid, F. X. (1989) in *Protein Structure: A Practical Approach* (Creighton, T. E., Ed.) pp 251–285, IRL Press, Oxford, U.K.
Shortle, D., Meeker, A. K., & Freire, E. (1988) *Biochemistry 27*, 4761–4768.
Smeaton, J. R., & Elliot, W. H. (1967) *Biochim. Biophys. Acta 145*, 547–560.
Stigter, D., Alonso, D. O. V., & Dill, K. A. (1991) *Proc. Natl. Acad. Sci. U.S.A. 88*, 4176–4180.
Stryer, L. (1965) *J. Mol. Biol. 13*, 482–495.
Sugawara, T., Kuwajima, K., & Sugai, S. (1991) *Biochemistry 30*, 2698–2706.
Tanford, C. (1968) *Adv. Protein Chem. 23*, 121–282.
Udgaonkar, J. B., & Baldwin, R. L. (1988) *Nature 335*, 694–699.
Wüthrich, K. (1986) *NMR of Proteins and Nucleic Acids*, Wiley, New York.